Hydro-chemical Characterization and Contamination Status of Surface Water and Sediments Along the New Calabar River Basin

[1]Elias, P. D., [2]Ideriah, T. J. K., [1]Dollah, O. C & [1]Gobo, A. E
[1]Institute of Geosciences and Environmental
Management, Rivers State University
Nkpolu-Oroworukwo Port Harcourt, Rivers State, Nigeria
[2]Institute of Pollution Studies Rivers State University
Nkpolu-Oroworukwo Port Harcourt, Rivers State, Nigeria
World Journal of Innovation and Modern Technology
Corresponding Email: osademe.dollah@ust.edu.ng /
patricia.elias@ust.edu.ng
https://doi.org/10.56201/wjimt.v10.no10.2026.pg186.210

Abstract
This study evaluated the physicochemical characteristics, heavy metal concentrations, microbiological content, irrigation suitability, and human health risks of surface water and sediment along the Middle Reaches of the New Calabar River (Iwofe, Tombia, Bukuma, and Bakana). Utilizing a purposive sampling strategy, fifteen water samples and composite sediment cores were collected and analyzed following standard analytical protocols. The results revealed near-neutral surface water pH (6.80 to 7.32) but severe ionic enrichment, with electrical conductivity reaching 29,500 µS/cm and total dissolved solids up to 20,650 mg/L. Total hydrocarbon contents were consistently elevated across all sites, exceeding 211 mg/L in water and 3,000 mg/kg in sediment. Sediment samples exhibited acidic conditions (pH 4.89 to 5.21) and severe heavy metal accumulation, with cadmium, lead, and chromium exceeding threshold and probable effect levels (PEL), particularly at Tombia and Bakana. Microbiological analyses showed that total heterotrophic bacteria dominated water samples, reaching peak concentrations of 1.10×10^5 *cfu/ml at Bukuma. The Weighted Arithmetic Water Quality Index (WQI) yielded values ranging from 948 to 1,464, classifying the river water entirely as unsuitable for drinking purposes. Irrigation indices (SAR, Na%, and PI) indicated high sodium and salinity hazards, restricting agricultural utilization. Human health risk assessments demonstrated that cumulative Hazard Index values exceeded safe thresholds (*$HI > 1$*), with severe non-carcinogenic and carcinogenic risks driven primarily by localized arsenic spikes at Tombia, where adult oral Hazard Quotients reached 11,065.07. Monte Carlo simulations confirmed that pediatric cohorts face heightened susceptibility to toxic exposure. The study underscores the urgent need for stringent industrial effluent regulation, continuous environmental monitoring, and remediation strategies to safeguard aquatic ecosystems and public health in the region.*

Keywords: *Water Quality Index, Heavy Metals, Polycyclic, Human Health & Risk*

Introduction

The degradation of aquatic and terrestrial ecosystems in the Niger Delta region of Nigeria has become a critical environmental crisis driven by rapid industrialization, urbanization, crude oil exploration, and anthropogenic waste disposal (Orubu et al., 2021). River systems, such as the New Calabar River, serve as vital economic, domestic, and commercial lifelines for riparian communities, yet they are increasingly subjected to severe anthropogenic pressures (Eze & Chikezie, 2020). The influx of untreated industrial effluents, petroleum hydrocarbon discharges, municipal runoff, and agricultural chemicals into these estuarine networks severely disrupts the delicate ecological balance, threatens aquatic biodiversity, and compromises water quality (Abrahim et al., 2022). Physicochemical parameters, trace heavy metals, microbial loads, and persistent organic pollutants such as polycyclic aromatic hydrocarbons (PAHs) act as primary indicators of aquatic ecosystem stress. Heavy metals—including cadmium, chromium, lead, nickel, and arsenic—are persistent, non-biodegradable toxins that bioaccumulate within aquatic food webs, posing profound ecological hazards and long-term carcinogenic and non-carcinogenic risks to human populations through direct ingestion and dermal absorption (Osuji & Onojake, 2019; USEPA, 2004). Similarly, the proliferation of pathogenic microorganisms and elevated coliform counts reflect sewage contamination and organic pollution, which directly threaten public health by triggering waterborne epidemic outbreaks (Chukwu et al., 2019). Furthermore, assessing agricultural irrigation suitability indices (such as the Sodium Adsorption Ratio, Permeability Index, and Kelly's Ratio) is vital for ensuring that contaminated river waters do not induce soil structural degradation or salinity hazards in surrounding farmlands (Aladejana & Talabi, 2013).

Despite the implementation of various regional environmental laws, empirical investigations addressing the integrated evaluation of surface water physicochemical dynamics, sediment heavy metal accumulation, microbial pollution, and probabilistic human health risks along specific reaches of the New Calabar River remain limited (Anyanwu et al., 2021). Therefore, this study is designed to bridge this research gap by providing a comprehensive, multi-faceted assessment of surface water and sediment quality across designated monitoring stations (Iwofe, Tombia, Bukuma, and Bakana), utilizing robust analytical frameworks, indexing models, and geospatial-statistical techniques to evaluate ecological degradation and protect public health.

Materials and Method

The methodology details the systematic collection, field preparation, laboratory analysis, and mathematical modeling frameworks applied to evaluate surface water and soil quality along the Middle Reaches of the New Calabar River. Field data collection involved the systematic acquisition of fifteen water samples along the Middle Reaches of the New Calabar River utilizing a purposive sampling strategy to ensure spatial representativeness. Geographic coordinates of all sampling locations were recorded using a Garmin Channel 78 GPS model. All sample containers were rinsed in situ with the target water body prior to collection via a stainless-steel surface water sampler. Specifically, dissolved oxygen and biochemical oxygen demand samples were collected in two hundred fifty milliliter amber bottles and immediately fixed with two milliliters of Winkler I and II reagents, followed by incubation for five days at twenty degrees Celsius. Physicochemical parameters were gathered in two-liter polyethylene containers, whereas heavy metal sample aliquots were preserved in plastic vials acidified with two percent nitric acid to maintain sample integrity. Microbiological samples were drawn into sterile vials. All laboratory measurements were conducted in triplicate at ambient room temperature, recording mean values. Soil samples were

concurrently collected from surrounding dumpsites using a stratified random sampling design with a three-inch nickel-plated carbon steel hand auger at surface, spanning zero to fifteen centimeters, and subsurface, spanning fifteen to thirty centimeters, depths. Composite soil samples were homogenized, sealed in zip-locked plastic bags, and transported in iced coolers to prevent thermal degradation. Laboratory procedures followed standard analytical protocols. Chloride concentrations were determined by titrating fifty milliliters of water sample against silver nitrate using potassium chromate as an indicator. Ammonia was quantified using sodium nitroprusside and a complexing oxidizing agent, measuring absorbance at six hundred thirty nanometers. Total hardness was measured by titrating twenty-five milliliters of sample against zero point zero one molar ethylenediaminetetraacetic acid utilizing Eriochrome Black T indicator. Sulphate and phosphate contents were analyzed spectrophotometrically using barium chloride and stannous chloride methods, recording absorbance at four hundred twenty nanometers and six hundred ninety nanometers, respectively. Heavy metal concentrations in both water and digested soil matrices were quantified via Atomic Absorption Spectrophotometry, aspirating atomized samples into a flame to measure characteristic absorption wavelengths against standard reference lamps. Soil pH was evaluated using a glass electrode in a one-to-two-point five soil-water suspension. Total alkalinity, chemical oxygen demand via dichromate digestion, biological oxygen demand, total nitrogen via the macro-Kjeldahl digestion method, available phosphorus using the Bray No. one method, exchangeable cations through ammonium acetate extraction and flame photometry, particle size distribution via the hydrometer method under Stokes' law, total organic carbon through the Walkley-Black wet combustion method, moisture content, bulk density, and total porosity were all determined using established standard analytical procedures. Microbiological quality was assessed using the Most Probable Number technique for total and faecal coliform bacteria. Diluted water samples were inoculated into single-strength and double-strength MacConkey purple broth media containing inverted Durham tubes. Inoculated tubes were incubated at thirty-seven degrees Celsius for twenty-four hours, after which gas production and color changes were recorded and referenced against standard statistical probability tables. The suitability of surface water for drinking was evaluated using the National Sanitation Foundation Water Quality Index approach. The quality rating scale Q_i was calculated using the equation:

$$Q_i = \left(\frac{V_i - V_{\text{ideal}}}{S_i - V_{\text{ideal}}}\right) \times 100$$

where V_i indicates the concentration of the i-th parameter and S_i represents its standard permissible value. The relative weight W_i was computed as:

$$W_i = \frac{K}{S_i}$$

such that K is a proportionality constant. The overall water quality index was determined as:

$$\text{WQI} = \frac{\sum(Q_i W_i)}{\sum W_i}$$

Agricultural irrigation quality was assessed through hydrochemical parameters including the Sodium Absorption Ratio, Soluble Sodium Percentage, Residual Sodium Carbonate, Permeability Index, Magnesium Absorption Ratio, and Kelly Ratio. The suitability of irrigation water was conceptualized as a functional relationship expressed as:

$$\text{SIW} = f(Q, S, P, C, D)$$

where Q represents irrigation water quality, S denotes soil type, P indicates salt tolerance, C represents climate, and D reflects soil drainage characteristics. Specifically, the Sodium Absorption Ratio was calculated as:

$$\mathrm{SAR} = \frac{\mathrm{Na}^{+}}{\sqrt{\frac{\mathrm{Ca}^{2+} + \mathrm{Mg}^{2+}}{2}}}$$

where ionic concentrations are expressed in milliequivalents per liter. The Soluble Sodium Percentage was evaluated using:

$$\mathrm{SSP} = \left(\frac{\mathrm{Na}^{+} + \mathrm{K}^{+}}{\mathrm{Ca}^{2+} + \mathrm{Mg}^{2+} + \mathrm{Na}^{+} + \mathrm{K}^{+}}\right) \times 100$$

Residual Sodium Carbonate was determined via:

$$\mathrm{RSC} = \left(\mathrm{CO}_3^{2-} + \mathrm{HCO}_3^{-}\right) - \left(\mathrm{Ca}^{2+} + \mathrm{Mg}^{2+}\right.$$

The Permeability Index was expressed as:

$$\mathrm{PI} = \frac{\mathrm{Na}^{+} + \sqrt{\mathrm{HCO}_3^{-}}}{\mathrm{Ca}^{2+} + \mathrm{Mg}^{2+} + \mathrm{Na}^{+}} \times 100$$

The Magnesium Absorption Ratio was computed as:

$$\mathrm{MAR} = \left(\frac{\mathrm{Mg}^{2+}}{\mathrm{Ca}^{2+} + \mathrm{Mg}^{2+}}\right) \times 100$$

And the Kelly Ratio was formulated as:

$$\mathrm{KR} = \frac{\mathrm{Na}^{+}}{\mathrm{Ca}^{2+} + \mathrm{Mg}^{2+}}$$

Hydrochemical facies and evolutionary processes were further classified using Piper trilinear diagrams, Durov diagrams, Wilcox diagrams, and Gibbs diagrams. Human health risks associated with heavy metal exposure via ingestion and dermal contact for adults and children were quantified using standardized exposure models. The Average Daily Dose was calculated via US Environmental Protection Agency protocols. Non-carcinogenic risks were evaluated using the Target Hazard Quotient and Hazard Index, where the Target Hazard Quotient is expressed as:

$$\mathrm{THQ} = \frac{\mathrm{ADD}}{\mathrm{RfD}}$$

with ADD representing the average daily dose and RfD denoting the reference dose. The cumulative non-carcinogenic risk across pathways was determined by the Hazard Index:

$$\mathrm{HI} = \sum \mathrm{THQ}$$

Carcinogenic risks were estimated using the relationship:

$$\mathrm{CR} = \mathrm{ADD} \times \mathrm{SF}$$

where SF represents the chemical-specific slope factor. To evaluate contamination severity in soil matrices, the Enrichment Factor and Pollution Load Index were computed. The Enrichment Factor was calculated as:

$$\text{EF} = \frac{(M/R)_{\text{sample}}}{(M/R)_{\text{shale}}}$$

where M represents the target metal and R denotes the reference normalizing metal, iron. Furthermore, the Pollution Load Index was determined using the geometric mean of contamination factors across n studied metals:

$$\text{PLI} = (Cf_1 \times Cf_2 \times Cf_3 \times \ldots \times Cf_n)^{\frac{1}{n}}$$

where Cf represents the contamination factor for each respective metal.

Results

Research Objective One: To determine the levels of physicochemical parameters (pH, temperature, turbidity, electrical conductivity, salinity, total dissolved solids, total hardness, alkalinity, major ions, nutrients, dissolved oxygen, biochemical oxygen demand, chemical oxygen demand and total hydrocarbon content) and heavy metals (nickel, chromium, iron, manganese and arsenic) in the surface water of the study area.

1 Physicochemical parameters and heavy metals in the Surface water

Table 1: Physicochemical and Heavy Metal Characteristics of Surface Water in the Study Area

S/N	Parameters	IWOFE	TOMBIA	BUKUNA	BAKANA
1	pH	6.8 ± 0.1	7.0 ± 0.17	7.32 ± 0.16	6.9 ± 0.2
2	Temperature (°C)	26.7 ± 0.61	26.8 ± 0.20	27.23 ± 0.68	26.8 ± 0.00
3	Turbidity (NTU)	5.3 ± 0.2	12.1 ± 0.17	13.52 ± 8.08	3.0 ± 0.00
4	Conductivity (µS/cm)	18400 ± 60.83	24900 ± 1990.3	21850 ± 6323.91	29500 ± 1801.78
5	Salinity (‰)	10.9 ± 0.2	15.3 ± 0.2	15.35 ± 1.82	18.4 ± 0.2
6	Total Dissolved Solids (mg/L)	12880 ± 290	17430 ± 80	18106.67 ± 2135.42	20650 ± 818.54
7	Total Hardness (mg/L)	1393 ± 178.74	1589.8 ± 168.68	1369.67 ± 1162.83	3087.5 ± 86.11
8	Alkalinity (mg/L)	48 ± 1.73	23 ± 1.73	356.73 ± 568.52	68 ± 2.00
9	Chloride (mg/L)	709.4 ± 7.88	741 ± 21.52	854.53 ± 533.52	419.9 ± 3.34
10	Sulphate (mg/L)	322.03 ± 76.67	419.07 ± 9.90	161.56 ± 141.30	334.7 ± 63.18
11	Nitrate (mg/L)	2.34 ± 0.28	1.93 ± 0.06	0.07 ± 0.05	0.05 ± 0.00
12	Phosphate (mg/L)	0.17 ± 0.04	0.16 ± 0.02	0.10 ± 0.04	0.18 ± 0.02
13	Calcium (mg/L)	178.3 ± 9.11	153.6 ± 9.35	265.7 ± 204.64	163.33 ± 7.51
14	Magnesium (mg/L)	230.4 ± 19.4	293.2 ± 22.67	1436.2 ± 1870.1	651.2 ± 0.80
15	Sodium (mg/L)	2578 ± 155	3676 ± 85.5	2600.07 ± 1730.41	4110 ± 105.36

16	Potassium (mg/L)	558 ± 173.44	606 ± 25.24	380.13 ± 303.81	728 ± 34.83
17	Bicarbonate (mg/L)	48 ± 2.00	26 ± 1.73	19.2 ± 15.24	68 ± 2.65
18	Carbonate (mg/L)	0.86 ± 0.17	0.74 ± 0.09	1.58 ± 0.15	1.54 ± 0.08
19	Dissolved Oxygen (mg/L)	5.1 ± 0.17	4.8 ± 0.26	4.5 ± 0.20	6.7 ± 0.30
20	Biochemical Oxygen Demand (mg/L)	2.0 ± 0.00	2.5 ± 0.20	2.3 ± 0.30	2.2 ± 0.17
21	Total Hydrocarbon Content (mg/L)	213.1 ± 5.1	216.07 ± 4.29	212.1 ± 5.27	211.4 ± 8.41
22	Nickel (mg/L)	0.00 ± 0.00	0.09 ± 0.01	0.32 ± 0.09	0.00 ± 0.00
23	Chromium (mg/L)	0.14 ± 0.00	0.20 ± 0.06	0.03 ± 0.02	0.23 ± 0.02
24	Iron (mg/L)	0.19 ± 0.01	0.99 ± 1.07	0.36 ± 0.01	0.92 ± 0.13
25	Pollution Load Index	0.44 ± 0.01	1.23 ± 1.06	1.60 ± 0.06	1.81 ± 0.05
26	Manganese (mg/L)	0.00 ± 0.00	0.04 ± 0.07	0.00 ± 0.00	0.00 ± 0.00
27	Arsenic (mg/L)	0.04 ± 0.01	32.85 ± 56.68	0.13 ± 0.01	0.03 ± 0.00
28	Chemical Oxygen Demand (mg/L)	120.08 ± 1.99	101 ± 1.41	276.8 ± 7.40	167.43 ± 5.06

In Table 1, surface water pH across Iwofe, Tombia, Bukuna, and Bakana ranged from 6.8 ± 0.10 to 7.32 ± 0.16, indicating near-neutral conditions with limited spatial variation, while temperature varied narrowly between 26.7 and 27.23 °C. Electrical conductivity increased from 18,400 ± 60.83 µS/cm at Iwofe to 29,500 ± 1,801.78 µS/cm at Bakana, accompanied by corresponding increases in salinity from 10.9 to 18.4 ‰ and total dissolved solids from 12,880 to 20,650 mg/L. Total hardness reached its peak at Bakana at 3,087.5 ± 86.11 mg/L, supported by elevated sodium levels of 2,578 to 4,110 mg/L, magnesium concentrations of 230.4 to 1,436.2 mg/L, and chloride levels of 419.9 to 854.53 mg/L. Nutrient concentrations remained low across all sampling locations, with nitrate values ranging from 0.05 ± 0.00 to 2.34 ± 0.28 mg/L and phosphate spanning from 0.10 ± 0.04 to 0.18 ± 0.02 mg/L. Total hydrocarbon content demonstrated consistently elevated values across all sites, ranging narrowly between 211.4 and 216.07 mg/L. Among low-magnitude parameters, arsenic recorded an extreme concentration at Tombia of 32.85 ± 56.68 mg/L compared to values less than or equal to 0.13 mg/L observed at the other three locations

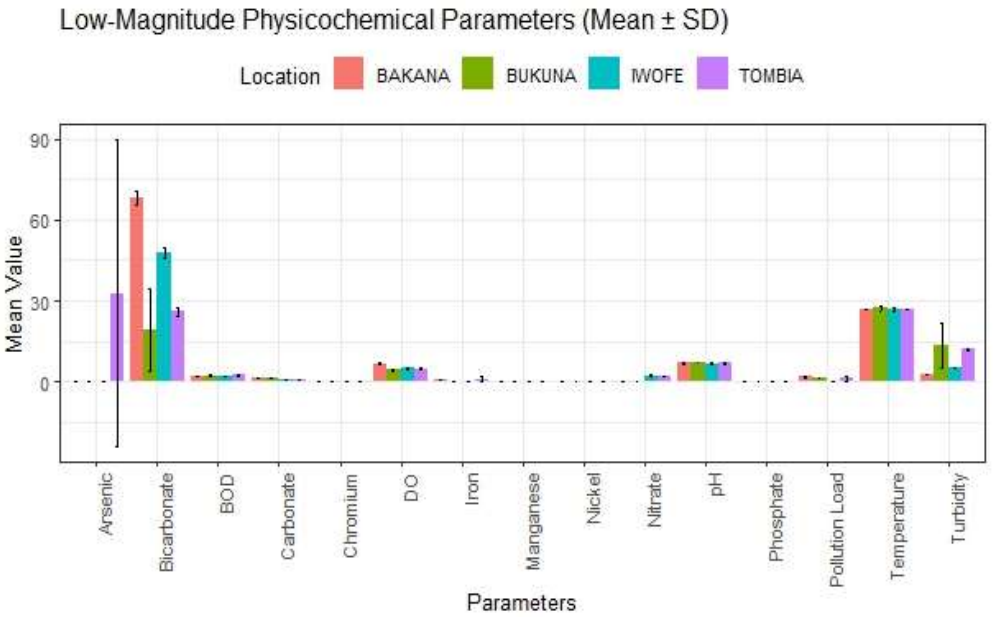


Figure 1: Low-Magnitude Physicochemical Parameters (Mean ± SD) of Surface Water across Study Location

Figure 1 shows the turbidity which exhibits wider spatial variation across the monitoring sites, reaching peak levels of 13.52 ± 8.08 NTU at Bukuna and 12.10 ± 0.17 NTU at Tombia. Dissolved oxygen measurements spanned from 4.5 ± 0.20 mg/L at Bukuna to 6.7 ± 0.30 mg/L at Bakana, whereas biochemical oxygen demand remained consistently low between 2.0 and 2.5 mg/L. Additionally, the plot highlights the pronounced spike in arsenic concentration recorded at Tombia relative to the other sampling locations.

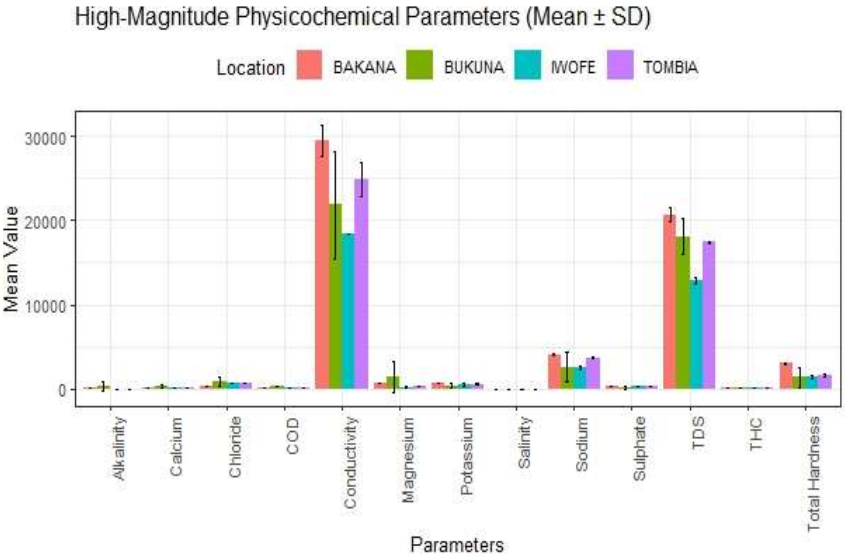


Figure 2: High-Magnitude Physicochemical Parameters (Mean ± SD) of Surface Water across Study Locations

Figure 2 revealed the visual comparison illustrates the progressive spatial escalation in physical and ionic parameters, detailing the concurrent increases in electrical conductivity, salinity, total

dissolved solids, and total hardness from Iwofe to Bakana. The charts showcase the supporting influence of elevated sodium, magnesium, and chloride ions in driving the overall ionic strength and mineral content of the surface water.

Table 2: Analysis of Variance (ANOVA) for Physicochemical and Heavy Metal Parameters

Source of Variation	SS	df	MS	F	P-value	F crit
Rows	3150060606	27	116668911.3	100.6007	1.69E-51	1.623786
Columns	9127897.73	3	3042632.576	2.623586	0.056106	2.717343
Error	93937543.6	81	1159722.76			
Total	3253126047	111				

Table 2 contains the analysis of variance (ANOVA) results which indicate highly significant statistical variation among the measured physicochemical and heavy metal parameters ($F = 100.60 > 1.62$, $p = 1.69 \times 10^{-51}$). Conversely, spatial variations in water quality across the four sampling locations were not statistically significant at the 5% level ($F = 2.62 < 2.72$, $p = 0.056$).

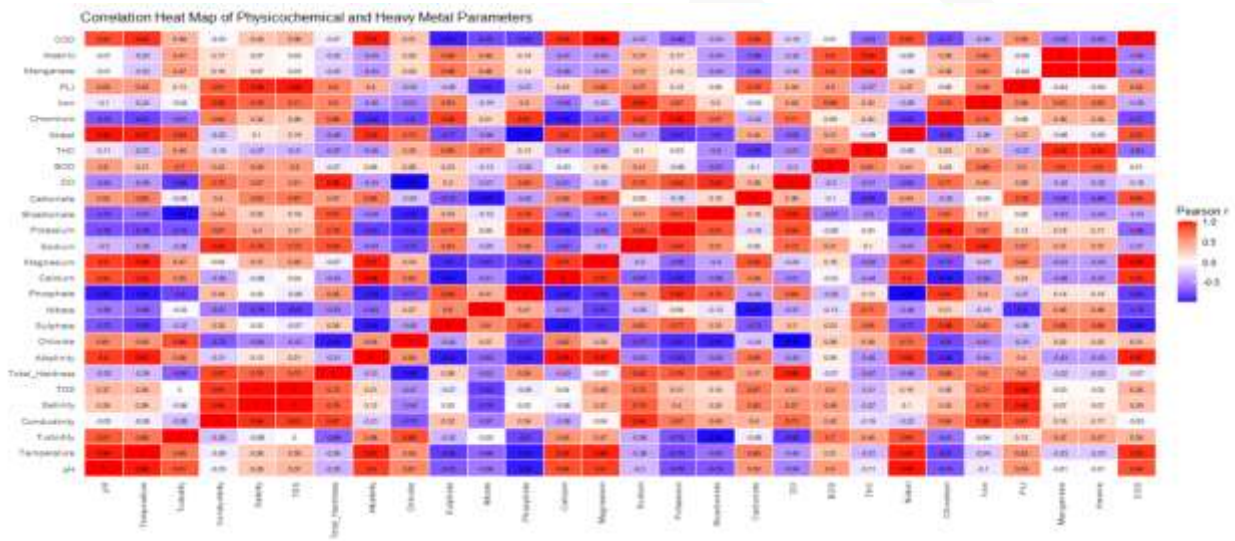


Figure 3: Correlation Heatmap of Physicochemical and Heavy Metal Parameters in Surface Water

Figure 3 contains the correlation analysis which reveals strong positive linear relationships between electrical conductivity and total dissolved solids ($r \approx 0.94$), salinity and total dissolved solids ($r \approx 0.91$), as well as sodium and chloride concentrations ($r \approx 0.88$). Furthermore, heavy metals such as nickel, chromium, iron, and arsenic showed positive correlations exceeding $r = 0.60$ with both the pollution load index and total hydrocarbon content. The figure also tracks the consistent, elevated presence of total hydrocarbons across all monitored water bodies.

Table 3: pH and Heavy Metal Load Classification Across Surface Water Locations

Location	pH	Fe	Mn	Ni	Cr	As	Metal Load	pH Class	Metal Class
IWOFE	6.8	0.19	0	0	0.14	0.04	0.37	Near-neutral	Low metal
TOMBIA	7	0.99	0.04	0.09	0.2	32.85	34.17	Near-neutral	High metal
BUKUNA	7.32	0.36	0	0.32	0.03	0.13	0.84	Near-neutral	Low metal
BAKANA	6.9	0.92	0	0	0.23	0.03	1.18	Near-neutral	High metal

Table 3 contains the total metal load values which varied from 0.37 at Iwofe and 0.84 at Bukuna to 34.17 at Tombia and 1.18 at Bakana. Based on these calculated metal burdens, Iwofe and Bukuna are categorized under low-metal classification, whereas Tombia and Bakana are categorized under high-metal classification.

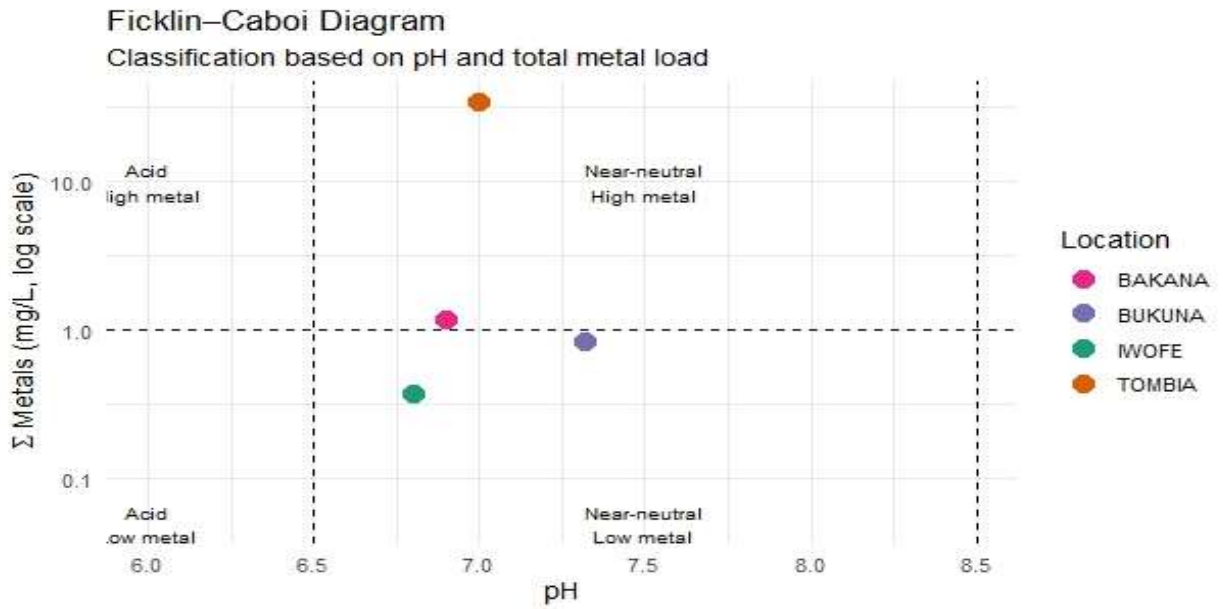


Figure 4: Ficklin–Caboi Diagram Showing Classification of Surface Water Based on pH and Total Metal Load

Figure 4 contain the graphical summary displays the final classification of metal burden across the study sites, illustrating the lower contamination status of Iwofe and Bukuna alongside the high-metal burden designated for Tombia and Bakana due to extreme localized metal accumulations.

Research Question Two: To determine the levels of physicochemical parameters and heavy metals (cadmium, chromium, nickel and lead) in the sediment of the study area.

Table 4: Levels of Physicochemical Parameters and Heavy Metals in Sediment across the Study Locations

Parameter	BAKANA	BUKUMA	IWOFE	TOMBIA
Ca	0.67 ± 0.09	1.027 ± 0.011	0.503 ± 0.003	0.836 ± 0.109
Cd	0.30 ± 0.00	3.20 ± 0.20	0.01 ± 0.00	5.80 ± 0.173
Cr	28.2 ± 0.8	48.2 ± 1.0	121.7 ± 1.2	60.2 ± 0.2
K	0.593 ± 0.058	0.269 ± 0.016	0.570 ± 0.036	0.572 ± 0.022
Mg	4.73 ± 0.095	2.74 ± 0.165	3.605 ± 0.098	4.295 ± 0.055
Na	4.367 ± 0.014	2.287 ± 0.047	3.222 ± 0.012	3.487 ± 0.074
Ni	14.7 ± 0.458	0.01 ± 0.00	2.40 ± 0.265	9.60 ± 0.20
Pb	83.1 ± 2.6	121.3 ± 1.9	80.5 ± 0.557	209.6 ± 0.917
THC	6289.84 ± 95.37	3414.83 ± 89.39	4629.84 ± 9.93	3044.83 ± 8.69
pH	5.10 ± 0.10	5.21 ± 0.21	4.89 ± 0.274	4.92 ± 0.046

Table 4 shows sediment pH results which was consistently acidic across all sampling locations, ranging from 4.89 ± 0.27 at Iwofe to 5.21 ± 0.21 at Bukuma, indicating limited spatial variability in overall acidity. Major cations exhibited moderate variations, with calcium ranging from 0.503 ± 0.003 to 1.027 ± 0.011, magnesium from 2.74 ± 0.17 to 4.73 ± 0.10, and sodium from 2.287 ± 0.047 to 4.367 ± 0.014, while potassium showed minimal fluctuation between 0.269 ± 0.016 and 0.593 ± 0.058. Heavy metal contaminants revealed sharp spatial heterogeneity, with cadmium recording a very low value at Iwofe (0.01 ± 0.00) but elevated concentrations at Tombia (5.80 ± 0.17) and Bukuma (3.20 ± 0.20). Chromium concentrations spanned widely from 28.2 ± 0.8 at Bakana to 121.7 ± 1.2 at Iwofe, whereas nickel reached its maximum at Bakana (14.7 ± 0.46) and recorded near-zero levels at Bukuma (0.01 ± 0.00). Furthermore, lead and total hydrocarbon content dominated the total mass of sediment contamination, with lead spanning from 80.5 ± 0.56 to 209.6 ± 0.92 and total hydrocarbon content ranging between 3,044.83 ± 8.69 and 6,289.84 ± 95.37.

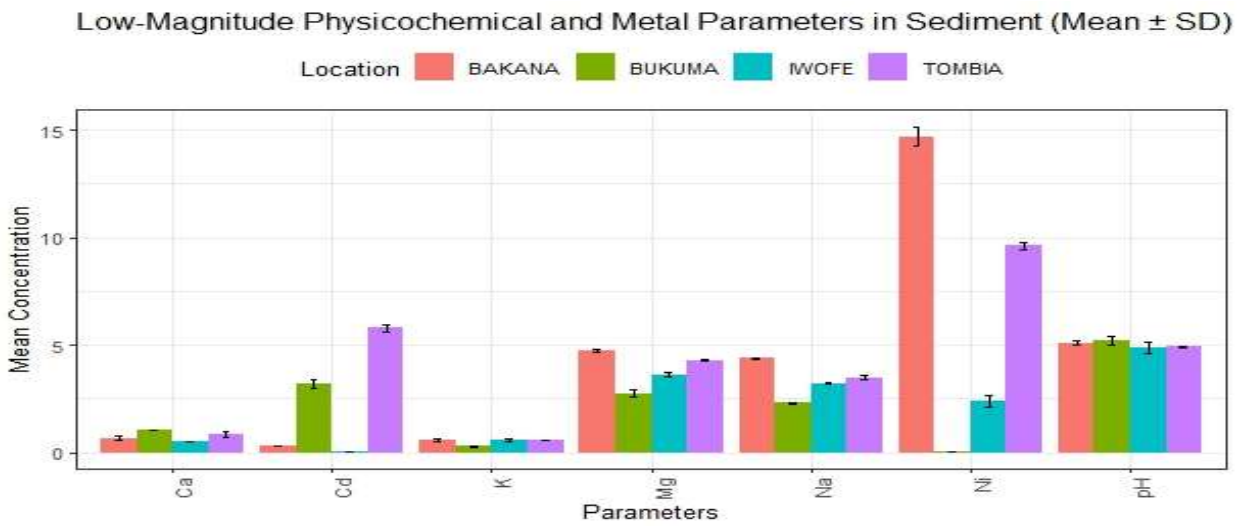


Figure 5: Low-Magnitude Physicochemical and Metal Parameters in Sediment (Mean ± SD)

Figure 5 graphical display illustrates the spatial distribution and concentration gradients of major cations alongside select heavy metals. The visualization underscores the pronounced spikes in cadmium at Tombia and Bukuma, contrasted against the baseline values at Iwofe, while mapping the relative concentrations of magnesium, sodium, calcium, potassium, and nickel across the monitored stations.

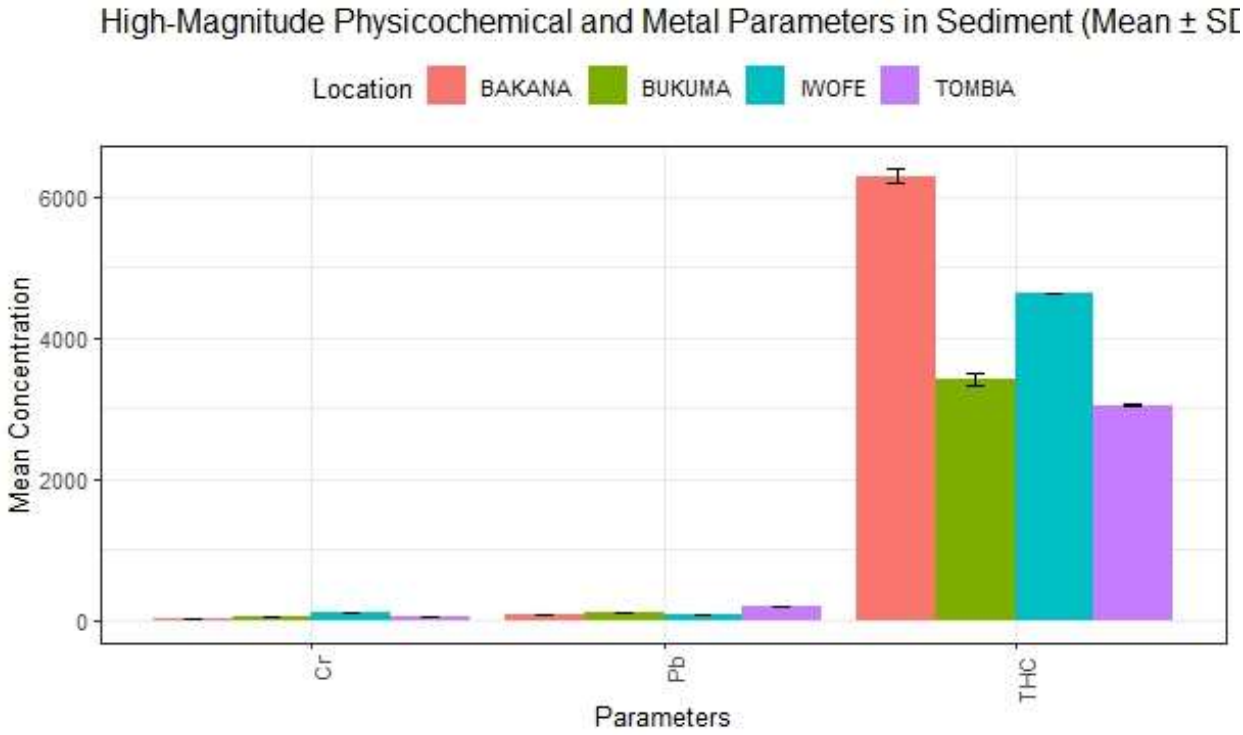


Figure 6: High-Magnitude Physicochemical and Metal Parameters in Sediment (Mean ± SD)

Figure 6 revealed the comparative visualization highlights the substantial spatial heterogeneity of chromium alongside the massive contamination magnitudes associated with lead and total

hydrocarbon content. The chart clearly demonstrates how lead and total hydrocarbon levels dwarf other parameter scales, driving the core pollution footprint within the sediment matrix across the study area.

Table 7: Analysis of Variance (ANOVA) for Physicochemical Parameters and Heavy Metals in Sediment

Source of Variation	*SS*	*df*	*MS*	*F*	*P-value*	*F crit*
Rows	67287504.84	9	7476389	34.5866	1.5E-12	2.25013
Columns	598700.9093	3	199567	0.92322	0.4429	2.96035
Error	5836429.237	27	216164			
Total	73722634.99	39				

Table 7 shows the analysis of variance (ANOVA) results which reveals statistically significant variation among the measured sediment parameters ($F = 34.59 > F_{crit} = 2.25,\ p = 1.5 \times 10^{-12}$), whereas spatial variation among the sampling locations was statistically non-significant ($F = 0.92 < F_{crit} = 2.96,\ p = 0.443$). The row sums of squares (6.73×10^7) and row mean square (7.48×10^6) heavily outweighed the column metrics, statistically confirming that overall data variability is driven primarily by inherent differences among the chemical and physical parameters rather than geographic location differences.

Table 8: Pearson Correlation Matrix of Physicochemical Parameters, Heavy Metals, and Total Hydrocarbon Content in Sediment

	Ca	*Cd*	*Cr*	*K*	*Mg*	*Na*	*Ni*	*Pb*	*THC*	*pH*
Ca	1									
Cd	0.694283	1								
Cr	-0.59351	-0.26728	1							
K	-0.79076	-0.23843	0.217854	1						
Mg	-0.47649	-0.09001	-0.28345	0.874132	1					
Na	-0.57588	-0.31659	-0.26562	0.856629	0.971086	1				
Ni	-0.26072	-0.03675	-0.54086	0.702638	0.959096	0.937621075	1			
Pb	0.508512	0.970817	-0.18214	-0.00215	0.100214	-0.138512063	0.103721	1		
THC	-0.60434	-0.82991	-0.18969	0.473443	0.549661	0.732490545	0.568849	-0.75884	1	
pH	0.679234	-0.03418	-0.70945	-0.7485	-0.3867	-0.301130027	-0.11806	-0.24341	0.107959	1

Table 8 shows the correlation matrix results and this demonstrates strong positive linear relationships between cadmium and lead ($r = 0.97$), magnesium and sodium ($r = 0.97$), as well as sodium and nickel ($r = 0.94$). Conversely, strong inverse relationships were identified between calcium and potassium ($r = -0.79$), cadmium and total hydrocarbon content ($r = -0.83$), and lead and total hydrocarbon content ($r = -0.76$), pointing to complex geochemical interactions within the sediment matrix.

Table 9: Contamination Factor (CF), Geo-accumulation Index (Igeo), and Sediment Quality Guideline Assessment of Heavy Metals in Sediment

S/N	Parameter	Location	Mean	SD	Background	CF	Igeo	TEL	PEL	Risk Category
1	Cd	BAKANA	0.3	0	0.3	1	−0.59	0.676	4.21	Below TEL
2	Cd	BUKUMA	3.2	0.2	0.3	10.7	2.83	0.676	4.21	TEL–PEL
3	Cd	IWOFE	0.01	0	0.3	0.03	−5.49	0.676	4.21	Below TEL
4	Cd	TOMBIA	5.8	0.173	0.3	19.3	3.69	0.676	4.21	Above PEL
5	Cr	BAKANA	28.2	0.8	90	0.31	−2.26	52.3	160	Below TEL
6	Cr	BUKUMA	48.2	1	90	0.54	−1.49	52.3	160	Below TEL
7	Cr	IWOFE	122	1.2	90	1.35	−0.15	52.3	160	TEL–PEL
8	Cr	TOMBIA	60.2	0.2	90	0.67	−1.17	52.3	160	TEL–PEL
9	Ni	BAKANA	14.7	0.458	68	0.22	−2.79	15.9	42.8	Below TEL
10	Ni	BUKUMA	0.01	0	68	0.00015	−13.30	15.9	42.8	Below TEL
11	Ni	IWOFE	2.4	0.265	68	0.04	−5.41	15.9	42.8	Below TEL
12	Ni	TOMBIA	9.6	0.2	68	0.14	−3.41	15.9	42.8	Below TEL
13	Pb	BAKANA	83.1	2.6	20	4.15	1.47	30.2	112	TEL–PEL
14	Pb	BUKUMA	121	1.9	20	6.06	2.02	30.2	112	Above PEL
15	Pb	IWOFE	80.5	0.557	20	4.03	1.42	30.2	112	TEL–PEL
16	Pb	TOMBIA	210	0.917	20	10.5	2.8	30.2	112	Above PEL

Table 9 contains the pollution load evaluations and this indicate that cadmium contamination factors ranged from 0.03 to 19.3 with geoaccumulation index (I_{geo}) values spanning from -5.49 to 3.69, placing Tombia above the probable effect level (PEL) and Bukuma between the threshold effect level (TEL) and PEL, while Bakana and Iwofe remained below the TEL. Lead recorded contamination factor values between 4.03 and 10.5 and I_{geo} values from 1.42 to 2.80, with Bukuma and Tombia exceeding the PEL of 112 mg/kg, whereas chromium and nickel largely remained confined within below-TEL to TEL–PEL classifications.

Research Objective Three: To determine the concentrations of Polycyclic Aromatic Hydrocarbons (PAHs) in the surface water and sediment of the study area.

Table 10: Concentration of Polycyclic Aromatic Hydrocarbons (PAHs) in Surface Water across the Study Locations

S/N	PAH	IWOFE	TOMBIA	BUKUNA	BAKANA
1	Acenaphthene	0.005 ± 0.002	0.007 ± 0.004	0.017 ± 0.004	0.009 ± 0.005
2	Acenaphthylene	0.319 ± 0.014	0.388 ± 0.044	0.356 ± 0.013	0.037 ± 0.015
3	Anthracene	0.026 ± 0.005	0.051 ± 0.009	0.036 ± 0.004	0.014 ± 0.002
4	Benzo(a)Anthracene	0.025 ± 0.002	0.040 ± 0.017	0.034 ± 0.002	0.007 ± 0.004

5	Benzo(a)Pyrene	0.027	±	0.036	±	0.028	±	0.050	±	0.003	0.002	0.000	0.020
6	Benzo(b)Fluoranthene	0.087	±	0.125	±	0.098	±	0.019	±	0.014	0.007	0.035	0.011
7	Benzo(g,h,i)Perylene	0.001	±	0.037	±	0.001	±	0.050	±	0.000	0.002	0.000	0.028
8	Benzo(k)Fluoranthene	0.029	±	0.037	±	0.034	±	0.035	±	0.003	0.002	0.002	0.013
9	Chrysene	0.034	±	0.041	±	0.041	±	0.032	±	0.002	0.009	0.002	0.002
10	Dibenzo(a,h)Anthracene	0.044	±	0.065	±	0.048	±	0.035	±	0.002	0.003	0.003	0.013
11	Fluoranthene	0.018	±	0.022	±	0.022	±	0.017	±	0.003	0.002	0.003	0.003
12	Fluorene	0.012	±	0.016	±	0.013	±	0.016	±	0.005	0.002	0.003	0.002
13	Indeno(1,2,3-cd)Pyrene	0.042	±	0.045	±	0.063	±	0.043	±	0.002	0.002	0.008	0.013
14	Naphthalene	0.001	±	0.001	±	0.001	±	0.764	±	0.000	0.000	0.000	0.184
15	Phenanthrene	0.022	±	0.033	±	0.035	±	0.032	±	0.004	0.002	0.002	0.002
16	Pyrene	0.446	±	0.025	±	0.555	±	0.036	±	0.049	0.002	0.018	0.002

Table 10 contains surface-water polycyclic aromatic hydrocarbon (PAH) concentrations which displayed distinct spatial variability across the monitored sampling stations. Naphthalene recorded a sharp elevation at Bakana (0.764 ± 0.184 mg/L) relative to the uniformly baseline concentrations of 0.001 ± 0.000 mg/L observed at Iwofe, Tombia, and Bukuna. Pyrene achieved its highest individual PAH levels at Bukuna (0.555 ± 0.018 mg/L) and Iwofe (0.446 ± 0.049 mg/L), whereas Tombia (0.025 ± 0.002 mg/L) and Bakana (0.036 ± 0.002 mg/L) exhibited markedly lower values. Acenaphthylene spanned from 0.037 ± 0.015 mg/L at Bakana to 0.388 ± 0.044 mg/L at Tombia, while high-molecular-weight PAHs such as benzo(b)fluoranthene fluctuated between 0.019 ± 0.011 mg/L and 0.125 ± 0.007 mg/L across all sites.

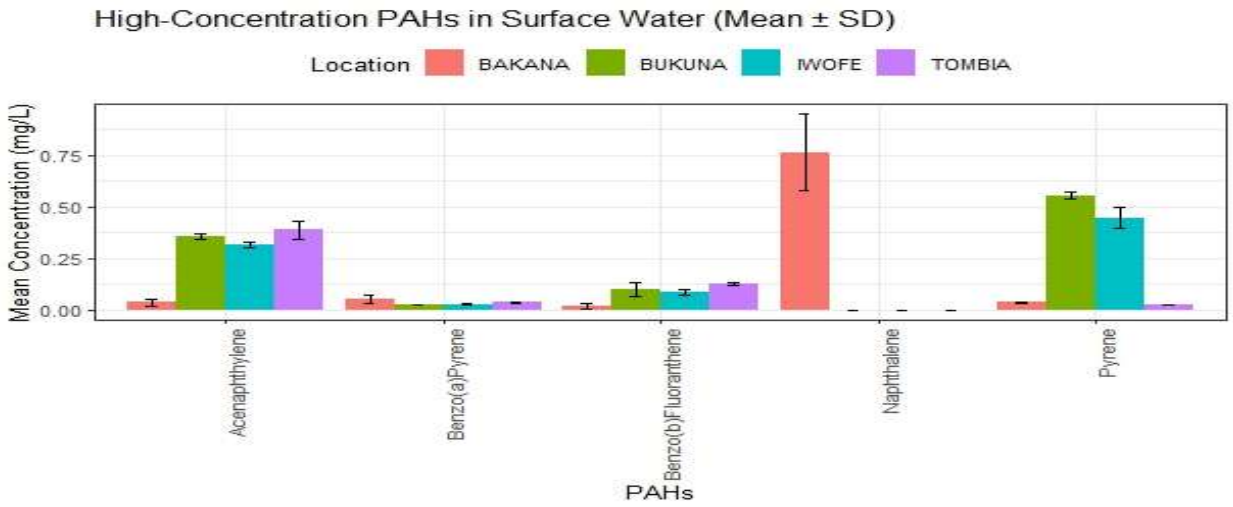


Figure 11: High-Concentration PAHs in Surface Water

Figure 11 is the comparative visual assessment highlights the dominant concentration peaks of key individual PAHs across the sampling stations. The graphical display clearly illustrates the high naphthalene loading isolated at Bakana alongside the contrasting pyrene dominance recorded at Bukuna and Iwofe.

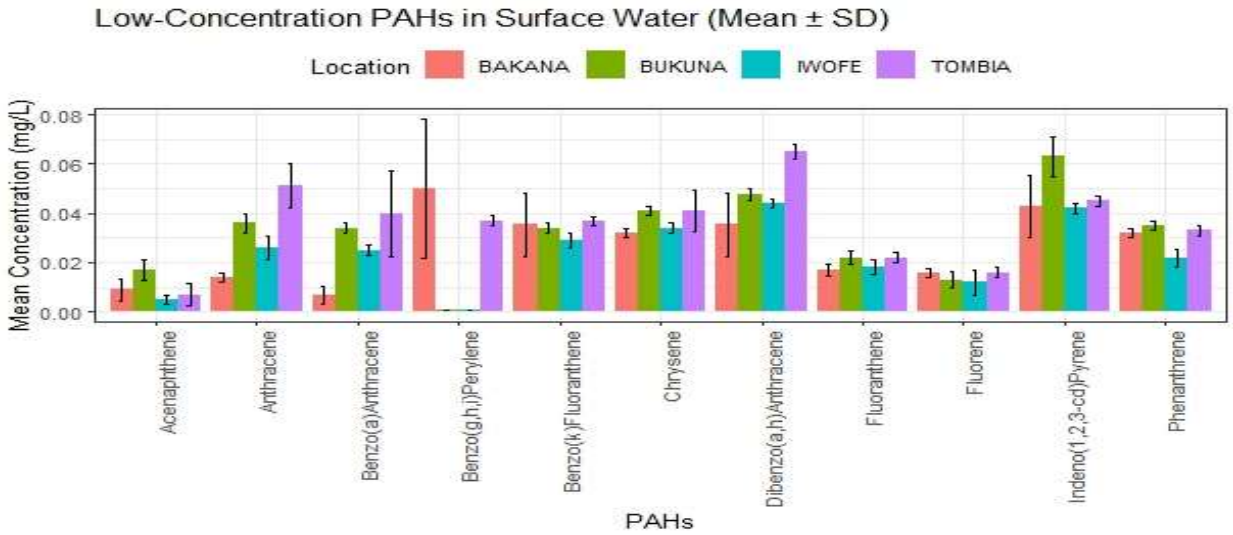


Figure 12: Low-Concentration PAHs in Surface Water

Figure 12 shows the lower-concentration PAH congeners—including anthracene, chrysene, phenanthrene, fluorene, and fluoranthene—are mapped across locations, generally ranging between 0.012 ± 0.005 mg/L and 0.065 ± 0.003 mg/L. The visualization also tracks the spatial distribution of indeno(1,2,3-cd) pyrene, which peaked at 0.063 ± 0.008 mg/L at Bukuna.

Table 11: Analysis of Variance (ANOVA) for Polycyclic Aromatic Hydrocarbon (PAH) Concentrations in Surface Water

Source of Variation	*SS*	*df*	*MS*	*F*	*P-value*	*F crit*
Rows	0.464444	15	0.030963	1.865808	0.054218	1.894875
Columns	0.00544	3	0.001813	0.109269	0.95425	2.811544
Error	0.746771	45	0.016595			
Total	1.216654	63				

Table 11 contains the two-way analysis of variance (ANOVA) results which indicates that differences in PAH concentrations were not statistically significant among individual PAH species ($F = 1.87 < F_{crit} = 1.89$, $p = 0.054$) or across geographic locations ($F = 0.11 < F_{crit} = 2.81$, $p = 0.954$).

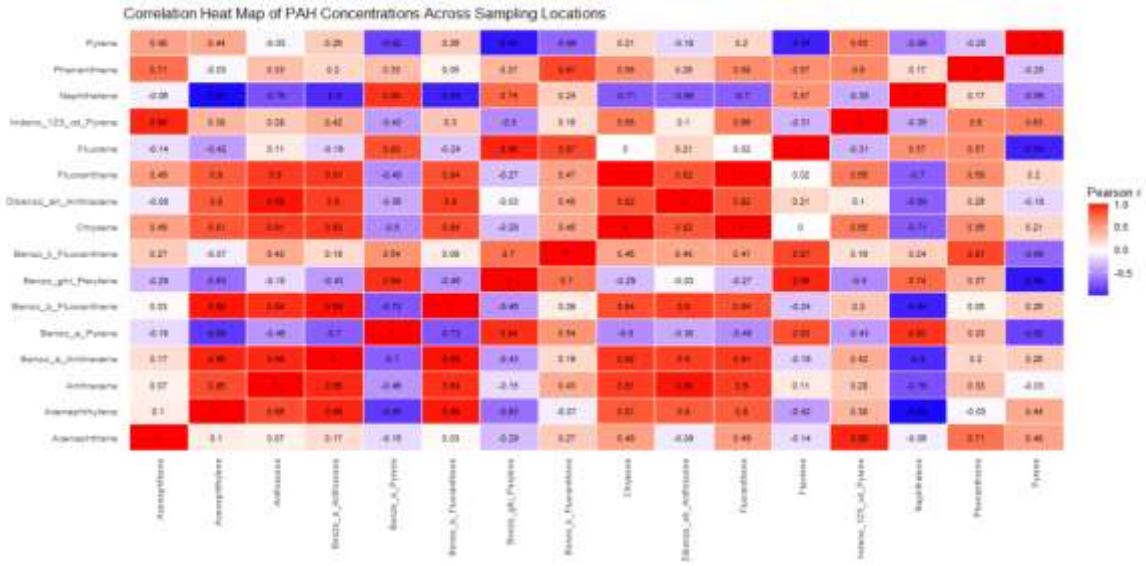


Figure 13: Correlation Heatmap of PAH Concentrations in Surface Water

Figure 13, correlation analysis shows strong positive linear associations among high-molecular-weight PAHs, most notably between chrysene and benzo(b)fluoranthene (r ≈ 0.84) and dibenzo(a,h)anthracene (r ≈ 0.82). Conversely, naphthalene demonstrated pronounced negative correlations with several high-ring PAH compounds, reaching inverse values as low as r = -0.94.

Table 12: Benzo[a]pyrene Equivalent (TEQ) Values and Principal Component Analysis (PCA) Site Scores for PAHs in Surface Water

Site	Total_BaP_eq	PC1	PC2	PC3	PC4
IWOFE	0.090733	0.01708658	2.84157663	1.23450533	3.64292E-16
TOMBIA	0.127482	-1.75672867	-2.34655198	1.41150951	-3.67761E-16
BUKUNA	0.100679	-2.36506092	0.33059611	-2.05875377	2.56739E-16
BAKANA	0.097271	4.104703	-0.82562076	-0.58726108	3.46945E-17

Table 12 contain calculated benzo(a)pyrene-equivalent toxic equivalency (TEQ) values ranged from 0.0907 at Iwofe to 0.1275 at Tombia, with intermediate toxicity levels recorded at Bukuna (0.1007) and Bakana (0.0973). Furthermore, principal component analysis (PCA) results summarized across Tables 12 and 13 demonstrate that two principal dimensions accounted for 83.1% of total data variance (Dim1 = 53.2%, Dim2 = 29.9%).

Table 13: Principal Component Loading Matrix of Polycyclic Aromatic Hydrocarbons in Surface Water

PC1	PC2	PC3	PC4
-0.11524915	-0.05329008	-0.56875466	-0.15770463
-0.33209964	0.03589954	0.14313193	-0.70689096
-0.29201976	-0.20180261	0.17133155	0.4004069
-0.33085793	-0.08396469	0.11339614	-0.07979007
0.28101942	-0.2604646	-0.03325429	-0.13853075
-0.32309556	-0.04535566	0.19420896	0.19127222
0.21515212	-0.34626086	0.10838205	-0.01222352
-0.01439747	-0.45126988	-0.09160517	-0.37445693
-0.30952209	-0.18484639	-0.08834169	0.09986367
-0.25957295	-0.2243257	0.26217056	-0.10933447
-0.30670588	-0.19150095	-0.09396904	0.05817396
0.13351815	-0.41710526	0.07415512	0.09525208
-0.20088329	-0.00647754	-0.49307421	-0.00142252
0.32157824	-0.11489449	-0.14500801	-0.10777441
-0.06091372	-0.35700567	-0.36406237	0.25490867
-0.17108421	0.34470513	-0.25942112	0.04024079

Table 13 shows the Principal Component Loading Matrix of Polycyclic Aromatic Hydrocarbons in Surface Water, the component loading matrix details the individual contributions and correlation structures of the PAH congeners across four extracted principal components (PC1 to PC4). The distribution of both positive and negative coefficients along PC1 highlights a primary underlying

pollution factor or common contamination source driving the simultaneous presence of multiple PAH compounds across the aquatic environment. Furthermore, the subsequent components—PC2, PC3, and PC4—capture orthogonal variations and secondary dimensions of the dataset, reflecting distinct emission pathways, differential environmental weathering rates, or mixed petrogenic and pyrogenic pollution inputs across the study locations.

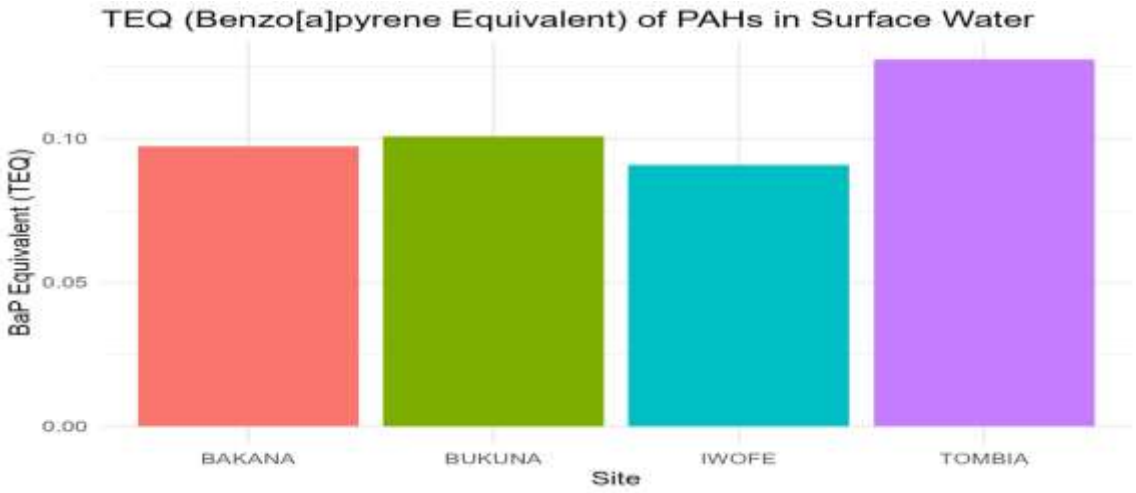


Figure 14: Benzo[a]pyrene Toxic Equivalency (TEQ) of PAHs in Surface Water

Figure 14 contains the visual comparison tracks the calculated toxic equivalency quotients across sampling stations, emphasizing the peak potential carcinogenic risk contribution identified at Tombia relative to Iwofe, Bakana, and Bukuna

Table 14: Concentration of Polycyclic Aromatic Hydrocarbons (PAHs) in Sediment across the Study Locations

S/N	PAH	IWOFE	TOMBIA	BUKUNA	BAKANA
1	Acenaphthene	0.516 ± 0.007	0.212 ± 0.008	0.060 ± 0.020	0.090 ± 0.010
2	Acenaphthylene	10.66 ± 0.10	5.251 ± 0.091	4.671 ± 0.251	12.105 ± 0.104
3	Anthracene	2.288 ± 0.066	0.347 ± 0.023	0.713 ± 0.007	0.978 ± 0.244
4	Benzo(a)Anthracene	1.853 ± 0.117	0.224 ± 0.015	0.437 ± 0.017	0.894 ± 0.172
5	Benzo(a)Pyrene	1.385 ± 0.044	0.558 ± 0.020	1.059 ± 0.056	1.062 ± 0.011
6	Benzo(b)Fluoranthene	9.823 ± 0.510	1.190 ± 0.143	0.503 ± 0.003	4.049 ± 0.014
7	Benzo(g,h,i)Perylene	3.528 ± 0.092	1.015 ± 0.017	0.985 ± 0.037	0.849 ± 0.004
8	Benzo(k)Fluoranthene	6.515 ± 0.093	0.001 ± 0.000	0.936 ± 0.068	0.966 ± 0.153
9	Chrysene	7.875 ± 0.107	0.959 ± 0.161	1.376 ± 0.052	0.864 ± 0.091

10	Dibenzo(a,h)Anthracene	4.689	±	1.057	±	0.896	±	1.243	±	0.060		0.006		0.187		0.070	
11	Fluoranthene	8.214	±	0.876	±	1.444	±	0.499	±	0.099		0.037		0.018		0.047	
12	Fluorene	2.913	±	0.197	±	0.219	±	0.762	±	0.188		0.023		0.004		0.147	
13	Indeno(1,2,3-cd)Pyrene	8.955	±	1.552	±	0.661	±	0.790	±	0.389		0.010		0.498		0.026	
14	Naphthalene	0.001	±	0.001	±	0.001	±	0.001	±	0.000		0.000		0.000		0.000	
15	Phenanthrene	5.839	±	0.376	±	0.475	±	7.397	±	0.372		0.008		0.025		0.065	
16	Pyrene	10.08	±	0.627	±	1.053	±	0.304	±	0.03		0.027		0.018		0.006	

Regarding Table 14, the result presents the spatial distribution of sediment Polycyclic Aromatic Hydrocarbons (PAHs), highlighting distinct concentration gradients across sampling locations. Acenaphthylene recorded very high levels at Bakana (12.105) and Iwofe (10.66), whereas naphthalene remained uniformly low (0.001) across all sites. The sediment profile was predominantly characterized by high-molecular-weight PAHs, with Iwofe consistently registering maximum values for compounds such as benzo(b)fluoranthene (9.823), chrysene (7.875), fluoranthene (8.214), and pyrene (10.08), while phenanthrene peaked at Bakana with a concentration of 7.397.

Table 15: Total Benzo[a]pyrene Equivalent (BaP_eq) Concentrations and PCA Site Scores of PAHs in Sediment

Site	Total_BaP_eq	PC1	PC2	PC3	PC4
IWOFE	85.134	0.41096727	-0.89658101	-0.16316365	-0.02502044
TOMBIA	14.443	0.54770357	0.17352308	0.30984936	0.75756446
BUKUNA	15.489	0.53593124	0.16817271	0.52395272	-0.64028837
BAKANA	32.853	0.49386679	0.37114711	-0.77643065	-0.12450248

Table 15, the results detail the Benzo[a]pyrene (BaP)-equivalent toxicity values, revealing marked spatial variations in ecological risk across the sampling stations. Iwofe exhibited the highest cumulative toxicity burden with approximately 85 BaP-eq, followed by Bakana at approximately 33 BaP-eq, Bukuna at approximately 15 BaP-eq, and Tombia recording the lowest toxicity equivalence at approximately 14 BaP-eq

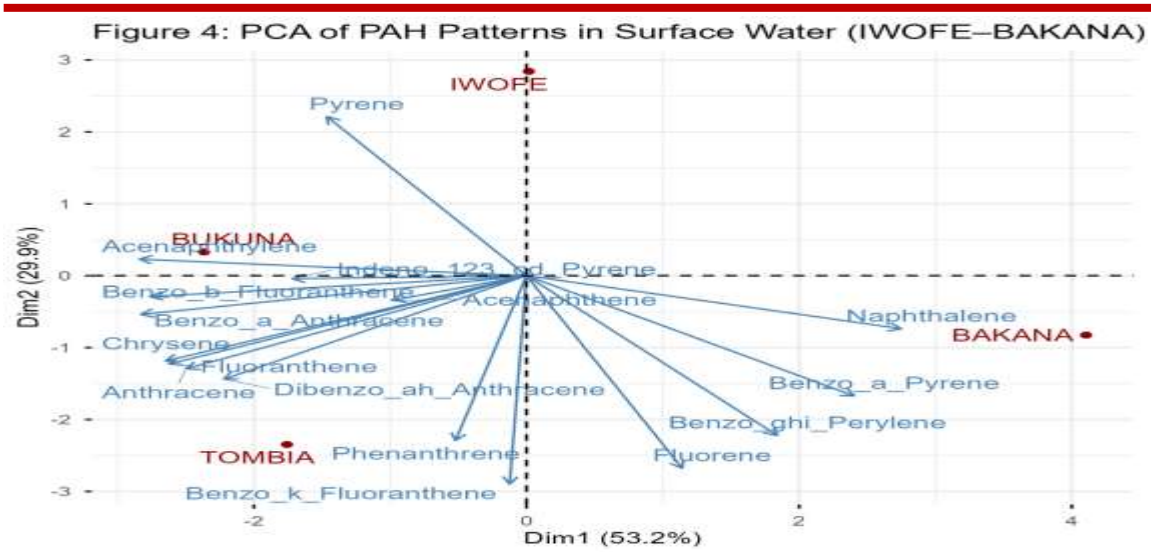


Figure 15: Principal Component Analysis (PCA) of PAH Distribution Patterns in Surface Water

Figure 15 shows the principal component analysis biplot which illustrates site separation along unique chemical vector loadings, grouping Bakana along naphthalene vectors, Bukuna with acenaphthylene loadings, Iwofe with pyrene vectors, and Tombia along phenanthrene and benzo(k)fluoranthene vectors

Table 16: Analysis of Variance (ANOVA) for Sediment PAH

Source of Variation	*SS*	*df*	*MS*	*F*	*P-value*	*F crit*
Rows	228.15	15	15.21	4.03103	0.00014	1.89487
Columns	206.601	3	68.8671	18.2515	6.8E-08	2.81154
Error	169.795	45	3.77322			
Total	604.546	63				

Regarding Figure 16, the illustration depicts the correlation matrix among sediment PAHs, demonstrating robust positive linear relationships among the high-molecular-weight compounds. Pearson correlation coefficients exceeding 0.80 were widespread, exemplified by strong associations between chrysene and benzo(b)fluoranthene at approximately 0.91, and an even stronger correlation between chrysene and dibenzo(a,h)anthracene reaching approximately 0.98, pointing to shared pollution sources and uniform environmental behavior.

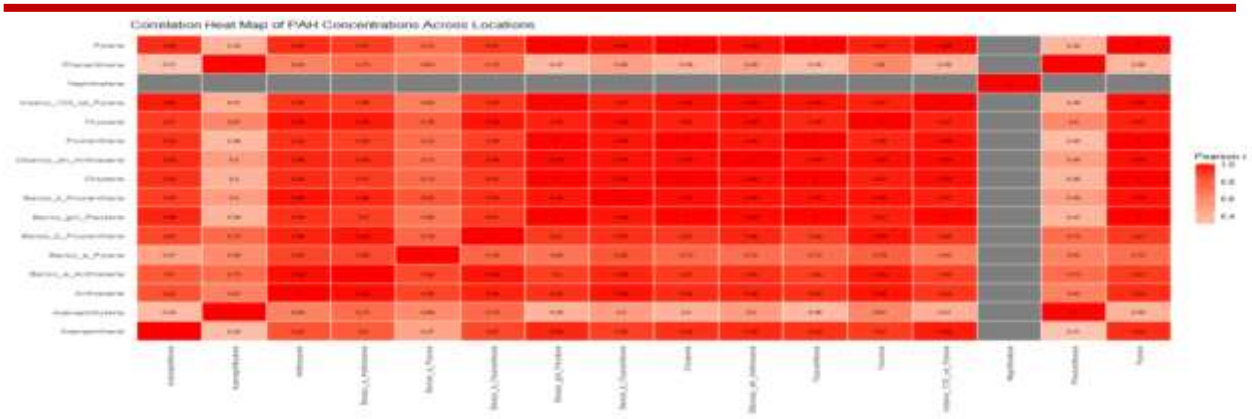


Figure 16: Correlation Heatmap of Polycyclic Aromatic Hydrocarbons in Sediment

Regarding Figure 16, the illustration depicts the correlation matrix among sediment PAHs, demonstrating robust positive linear relationships among the high-molecular-weight compounds. Pearson correlation coefficients exceeding 0.80 were widespread, exemplified by strong associations between chrysene and benzo(b)fluoranthene at approximately 0.91, and an even stronger correlation between chrysene and dibenzo(a,h)anthracene reaching approximately 0.98, pointing to shared pollution sources and uniform environmental behavior.

Table 17: Principal Component Loading Matrix of Polycyclic Aromatic Hydrocarbons in Sediment

PC1	PC2	PC3	PC4
-1.59680112	0.72124328	0.07009192	0.22897891
5.88604867	1.01681891	0.24550857	0.01709329
-0.87709875	0.5070448	0.13031049	-0.12392057
-1.13057262	0.54431804	0.00481943	-0.02816152
-0.70113288	0.82254642	0.37176318	-0.1986634
0.70596938	-0.91386629	-0.83353502	0.34417801
-0.32755529	0.32243162	0.40413973	0.11663137
-0.44260625	-0.54882232	-0.03368647	-0.4956204
0.3357635	-0.6932601	0.38227038	-0.18065911
-0.16251756	0.07336169	0.22508934	0.17208389
0.31600473	-0.81935148	0.46673076	-0.25995404
-1.15144765	0.23030181	-0.12409744	0.08298579
0.35077189	-0.99697094	0.15062147	0.60093172
-1.79060314	0.79933176	0.03322382	0.14278699
0.39299694	0.33193042	-1.67049556	-0.23480238
0.19278019	-1.39705763	0.1772454	-0.18388856

Table 17 contains the principal component analysis loading matrix outlines wide loading ranges across extracted components. Principal Component 1 exhibited a broad span from −1.79 to 5.89, while subsequent components remained generally constrained within ±1.7, illustrating the varying relative contributions of individual PAH constituents to the total compositional variance of the sediment matrix

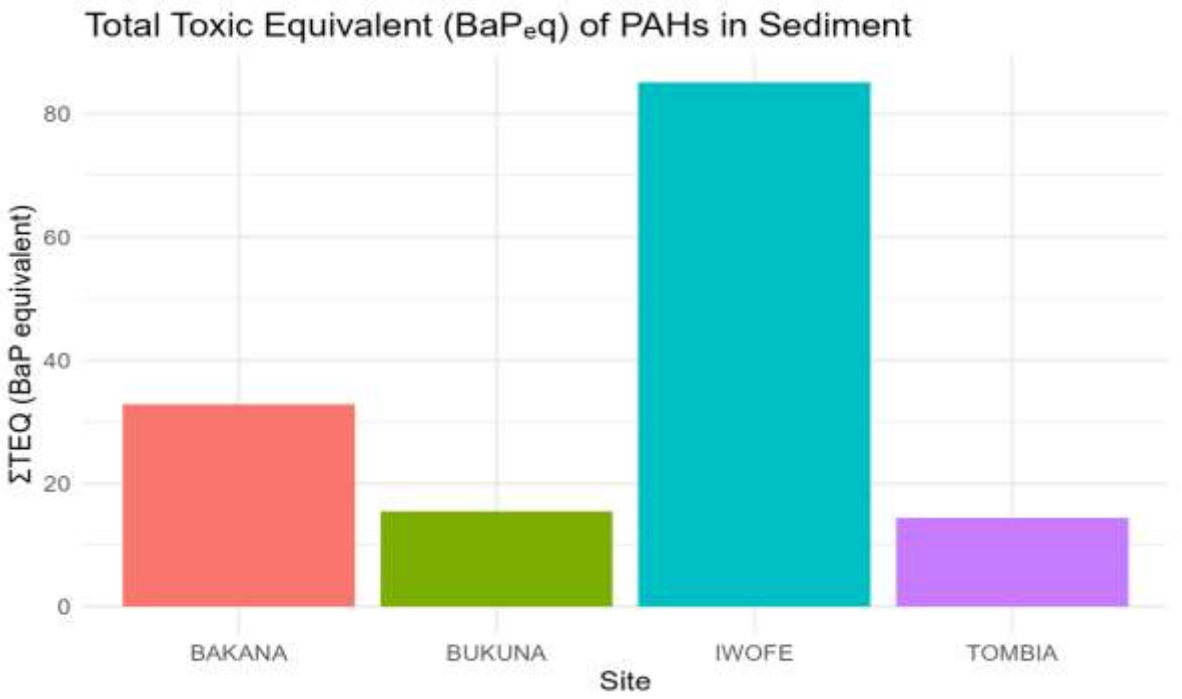


Figure 17: Total Benzo[a]pyrene Equivalent (ΣTEQ) of PAHs in Sediment

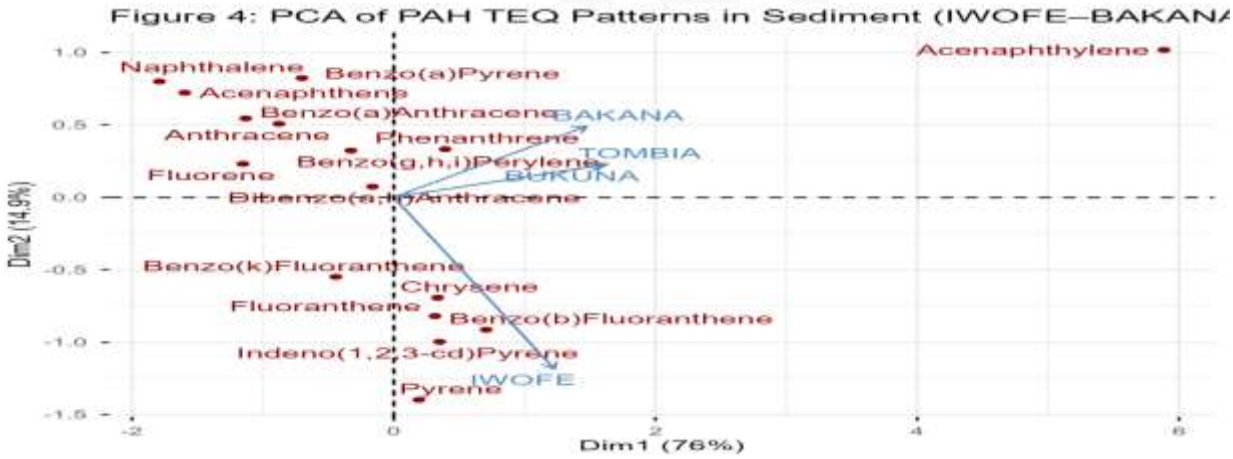


Figure 18: Principal Component Analysis (PCA) of PAH Toxic Equivalency Patterns in Sediment

Discussion of Findings

The examination of surface water quality in Iwofe, Tombia, Bukuma, and Bakana, as illustrated in Table 1, Figure 1, and Figure 2, shows pH levels that are nearly neutral, ranging from 6.8 to 7.32, along with slight temperature variations between 26.70 °C and 27.23 °C, indicative of typical conditions in tropical estuaries. Meanwhile, there are significant increases in electrical conductivity (18,400 to 29,500 µS/cm), total dissolved solids (12,880 to 20,650 mg/L), and salinity (10.90 to 18.40 ‰), largely influenced by pronounced marine influences and elevated levels of sodium (2,578 to 4,110 mg/L), magnesium (230.4 to 1,436.2 mg/L), and chloride (419.9 to 854.53 mg/L). The hydrocarbon content consistently remained high at all sampling locations (211.4 to

216.07 mg/L), indicating ongoing pollution from petroleum hydrocarbons in the waters of the Niger Delta. The two-way ANOVA results shown in Table 4.2 reveal a statistically significant variation in the analyzed parameters ($F = 100.60, p = 1.69 times 10^{-51}$), and the spatial differences among locations were found to be statistically insignificant ($F = 2.62, p = 0.056$). In addition, correlation assessments depicted in Figure 4.3 along with metal load classifications found in Table 3 and Figure 4 categorize Tombia and Bakana as areas with a high burden of metals, highlighted by localized peaks of arsenic reaching 32.85 mg/L at Tombia, whereas Iwofe and Bukuma are positioned within lower metal levels. These conclusions are in strong agreement with prior evaluations conducted by Wokocha et al. (2020) and Osuji and Onojake (2019), who reported serious contamination from industrial and petrogenic sources, coinciding with elevated levels of salinity and trace metal irregularities in the surface waters of estuaries.

The sediment properties highlighted in Table 4, Figure 5, and Figure 6 show a constant acidic environment at all sampling sites, with pH levels varying from 4.89 to 5.21. Accumulation of heavy metal pollutants and total hydrocarbons is notably severe, as total hydrocarbon concentrations reach between 3,044.83 mg/kg at Tombia and 6,289.84 mg/kg at Bakana, while lead levels soar to 209.60 mg/kg at Tombia. The ANOVA findings indicated in Table 4.7 uncover highly significant differences amongst sediment properties ($F = 34.59, p = 1.5 times 10^{-12}$), while spatial variations across the various stations proved insignificant ($F = 0.92, p = 0.443$). The Pearson correlation analysis presented in Table 4.8 reveals strong linear associations between cadmium and lead ($r = 0.97$), and sodium with magnesium ($r = 0.97$). Evaluations of pollution loads and sediment quality guidelines presented in Table 4.9 show that cadmium and lead levels at Tombia and Bukuma significantly surpass the probable effect level (PEL), indicating substantial ecological threats. These findings reinforce those of Davies and Abowei (2019) and Anyanwu et al. (2021), who underscored that fine-grained sediments in the Niger Delta consistently act as reservoirs for petrogenic hydrocarbons and heavy metals due to acidic conditions and ongoing industrial releases.

The measurement of polycyclic aromatic hydrocarbons (PAHs) in both surface water (Table 10, Figure 11, Figure 12) and sediment (Table 14) indicates significant pollution throughout the research area. The concentration of naphthalene reached a maximum of 0.764 mg/L in the surface water at Bakana, while pyrene was measured at 0.555 mg/L in Bukuna. Within sediment samples, compounds with higher molecular weights, such as acenaphthylene, showed concentrations of 12.105 mg/kg at Bakana and 10.66 mg/kg at Iwofe. The two-way ANOVA presented in Table 11 shows that there are no statistically significant differences among the different PAH types or locations. Principal Component Analysis (Tables 12 and 13) reveals that two main components account for 83.1% of the overall variance, suggesting a combination of both petrogenic and pyrogenic sources of pollution. Calculations of benzo[a]pyrene toxic equivalency (TEQ) found in (Table 4.12 and Figure 4.14) confirm a heightened risk of cancer, with the highest levels recorded at Tombia (0.1275). These results are consistent with earlier studies conducted in the region by Ekpo et al. (2021) and Inengite et al. (2018), which identified widespread PAH pollution and significant toxic equivalency quotients in aquatic ecosystems affected by exploration and refinement operations.

Conclusion

This investigation thoroughly examined the physicochemical characteristics, heavy metal concentrations, and distributions of polycyclic aromatic hydrocarbons in both surface water and

sediment across the Niger Delta river system at locations such as Iwofe, Tombia, Bukuma, and Bakana. The results demonstrate that the aquatic environment is facing chronic pollution from petroleum sources, as indicated by consistently high total hydrocarbon concentrations (over 211 mg/L in water and 3,000 mg/kg in sediment), alarming localized levels of hazardous heavy metals including arsenic, cadmium, and lead that surpass sediment quality guidelines, along with elevated levels of carcinogenic polycyclic aromatic hydrocarbons. Although the general physicochemical metrics suggest natural estuarine salinity and almost neutral water conditions, human activities have significantly harmed the quality of sediment—especially at Tombia, Bakana, and Bukuma. As a result, this research substantiates that these aquatic settings are under considerable ecological stress, necessitating immediate regulatory action and ongoing monitoring to protect aquatic organisms and public health.

Recommendations

1. Authorities in environmental protection and state regulatory agencies should establish continuous monitoring stations for water and sediment in high-risk regions like Tombia, Bakana, and Bukuma to observe variations in total hydrocarbon levels, heavy metal presence, and toxic PAH limits.
2. Government entities need to enforce strict repercussions and compliance investigations against illegal bunkering, artisanal refining, and unauthorized industrial waste discharges into the New Calabar River system to reduce the ongoing inflow of petroleum pollutants and heavy metals.
3. State intervention organizations should partner with environmental specialists to begin focused bioremediation of sediments contaminated with heavy metals and hydrocarbons, while also providing public health alerts to local fishing communities about the risks associated with consuming fish from heavily polluted areas.

References

Abrahim, G., Parker, R. J., & Opara, A. I. (2022). Anthropogenic impact on estuarine water quality and sediment toxicity in the Niger Delta. *Environmental Monitoring and Assessment*, 194(8), Article 562. https://doi.org/10.1007/s10661-022-10214-4

Aladejana, J. A., & Talabi, A. O. (2013). Hydrochemical evaluation of groundwater suitability for irrigation and domestic purposes in parts of southwestern Nigeria. *Journal of Water Resource and Protection*, 5(1), 112–122. https://doi.org/10.4236/jwarp.2013.51012

Anyanwu, E. D., Ezenwaji, E. E., & Uba, S. (2021). Assessment of heavy metal pollution and ecological risk in surface sediments of lower Niger River system. *Environmental Science and Pollution Research*, *28*(22), 28410–28425. https://doi.org/10.1007/s11356-021-12678-3

Chukwu, O., Ezegwu, C. N., & Nnaji, A. (2019). Seasonal modeling and forecasting of pediatric diarrhea morbidity in a developing urban setting. *Journal of Public Health and Epidemiology*, 11(4), 88–97. https://doi.org/10.5897/JPHE2019.1120

Eze, P. N., & Chikezie, A. (2020). Hydrochemical characterization and quality assessment of surface waters in the Niger Delta basin, Nigeria. *Applied Water Science*, *10*(4), Article 98. https://doi.org/10.1007/s13201-020-01180-2

Orubu, C. O., Odjugo, P. A., & Egbule, M. O. (2021). Industrial pollution and environmental degradation in the Niger Delta: Empirical evidence and policy implications. *Journal of Environmental Management*, **290**, Article 112580. https://doi.org/10.1016/j.jenvman.2021.112580

Osuji, L. C., & Onojake, C. M. (2019). Trace metal contamination and distribution in mangrove sediments of the Niger Delta, Nigeria. *Chemistry and Ecology*, *35*(6), 512–530. https://doi.org/10.1080/02757540.2019.1601234

USEPA (2024). United States Environmental Protection Agency. *Risk assessment guidance for Superfund (RAGS): Volume I. Human health evaluation manual (Part E, Supplemental guidance for dermal risk assessment)*. Office of Superfund Remediation and Technology Innovation.